Broadband Electromagnetic Detection and Discrimination of Underwater UXO (1321)

Final Report

Submitted to

Strategic Environmental Research and Development Program (SERDP)

August 31, 2005

By

Geophex, Ltd.
605 Mercury Street
Raleigh, NC 27603-2343

(919) 839-8515

Principal Investigator
Drs. Bill San Filipo and I.J. Won
sanfilipo@geophex.com

Report Documentation Page

Form Approved
OMB No. 0704-0188

1. REPORT DATE	2. REPORT TYPE	3. DATES COVERED
31 AUG 2005	**Final**	**-**

4. TITLE AND SUBTITLE	5a. CONTRACT NUMBER
Broadband Electromagnetic Detection and Discrimination of Underwater UXO	5b. GRANT NUMBER
	5c. PROGRAM ELEMENT NUMBER
6. AUTHOR(S) **San Filipo, Bill Won, I.J.**	5d. PROJECT NUMBER **MM-1321**
	5e. TASK NUMBER
	5f. WORK UNIT NUMBER
7. PERFORMING ORGANIZATION NAME(S) AND ADDRESS(ES) **Geophex, Ltd. 605 Mercury Street Raleigh, NC 27603-2343**	8. PERFORMING ORGANIZATION REPORT NUMBER
9. SPONSORING/MONITORING AGENCY NAME(S) AND ADDRESS(ES) **Strategic Environmental Research & Development Program 901 North Stuart Street, Suite 303 Arlington, VA 22203**	10. SPONSOR/MONITOR'S ACRONYM(S) **SERDP**
	11. SPONSOR/MONITOR'S REPORT NUMBER(S)

12. DISTRIBUTION/AVAILABILITY STATEMENT
Approved for public release, distribution unlimited

13. SUPPLEMENTARY NOTES
The original document contains color images.

14. ABSTRACT

15. SUBJECT TERMS

16. SECURITY CLASSIFICATION OF:			17. LIMITATION OF ABSTRACT	18. NUMBER OF PAGES	19a. NAME OF RESPONSIBLE PERSON
a. REPORT **unclassified**	b. ABSTRACT **unclassified**	c. THIS PAGE **unclassified**	**UU**	**30**	

Standard Form 298 (Rev. 8-98)
Prescribed by ANSI Std Z39-18

Table of Contents

Acronyms

CCR ..... Current Channeling Response
ECR ..... Eddy Current Response
EMI ..... Electromagnetic Induction
EMIS ..... Electromagnetic Induction Spectroscopy
ROC ..... Receiver Operator Characteristic
Pd ..... Probability of Detection
Pfa ..... Probability of False Alarm
SERDP ..... Strategic Environmental Research and Development Program
snr ..... signal/noise ratio
UXO ..... Unexploded Ordnance

Figures

Tables

Acknowledgements

This project was funded by the Strategic Environmental Research and Development Program (SERDP) under contract DACA72-02-C0026. The work was performed wholly by Geophex personnel; Steve Norton developed the modeling Algorithms and provided initial model studies; Bill SanFilipo performed the experiments with the help of Haoping Huang, Steve Norton, and Dak Darbha; Bill SanFilipo performed the data analysis and associated modeling. I.J. Won provided support and critical oversight. Drs. Jeff Marqusee and Anne Andrews, and the review committee for SERDP, provided support and constructive reviews during the course of the project.

Executive Summary

We addressed the environmental problem of unexploded ordnance (UXO) contamination in coastal areas where either practice range activity or ship-loading accidents (or intentional dumping) resulted in ordnance on or buried under bottom sediments. Not only is new or modified technology needed to cope with the logistic and acquisition complexities associated with the marine setting, but an understanding of the effects of the seawater on sensor data normally used in terrestrial missions is paramount before we attempt to use these sensors in seawater. This is particularly true when we attempt to analyze the data for clutter discrimination, where we use features in the data to characterize the target.

The scientific questions we explored focused on studying the underlying phenomenology of multi-frequency EMI measurements of UXO-like targets made in a conductive host medium. We have addressed this issue both with computer model algorithms and experiments so that we can understand how the multi-frequency EMI response in seawater differs from the free-air response (noting that the response of UXO buried in the ground generally consists of a simple superposition of the free-air response and background).

Computer algorithms we developed and used included finitely conducting, permeable sphere embedded in a conductive host and excited by a magnetic dipole transmitter, a modification to include a shell surrounding the sphere having different conductivity and permeability, and a perfectly conducting or insulating spheroid in a conductive medium and excited by a uniform applied field. These were used to quantify the effects of the seawater in terms of propagation distortion of the eddy current response (ECR) from the free-air response and the current channeling response (CCR) that only exists in the presence of a conductive medium. We also wrote an algorithm to compute the background response of seawater and the air (or bottom) interface. This provided information on background perturbation induced noise and apparent drift from depth changes.

We performed three sets of underwater experiments and corresponding control free-air measurements to confirm the computer models and to investigate seawater effects for UXO-like targets (pipes) not amenable to computer modeling. CCR was shown to be highly dependent on sensor-target geometry, and having a magnitude that increases with frequency so that it is generally important only above 10 kHz. We also found that surface corrosion or paint can drastically suppress or alter the CCR. In fact, if the target is completely insulated from the water, the CCR changes sign and has a magnitude of about one-half that of a conductor with good electrical contact with the water.

Details of much of the above work have been submitted in Quarterly Progress Reports, the Annual Reports, and presented at the IPR meetings and the SAGEEP conference. The conclusions from this work are that the CCR provides only marginal increase in detection footprint and is subject to condition and position of the target, and that the CCR may distort the spectral character of a target at high frequencies if the geometry and surface condition are right. We also have shown that the high frequencies are subject to noise induced by waves (if the sensor is not deep), and potentially noise associated with senor motion relative to the bottom, both as a result of perturbations to the large background response of seawater.

We employed our electromagnetic induction spectroscopy (EMIS) techniques on the data collected in the second experiment, using several pipes and spheres as known targets and a single "unknown" clutter item (metal paint tray). Based on what we had learned about CCR and propagation distortion of the spectra, we excluded the highest frequencies, limiting the range from 90 Hz to 11430 Hz or 5850 Hz. Noting that the distortion affects the quadrature more than inphase, we also tried applying different windows to each. The results are encouraging; in most cases where the offset distance was within a half meter, the correct identification was achieved, and the clutter item misfit was greater than almost all of the actual targets.

The final experiment was the most comprehensive and controlled; we performed it at the end of the project and are reporting results for the first time here. We collected spectra over a 2-dimensional grid at 20 cm intervals, for seven surrogate UXO of various sizes, and seven clutter items. The frequency band collected was limited to 21960 Hz and we windowed the range for the quadrature based on what we had learned (we used ten frequencies spaced somewhat closer than typical for terrestrial missions). Using free-air library spectra, we applied EMIS based identification, with clutter classification determined by a misfit threshold. Similar data were collected in air for a control and processed in the same way. We also processed the free-air spectra as we normally would for terrestrial surveys - using all frequencies (i.e. no quadrature frequency windowing) for comparison.

We generated receiver operator characteristic (ROC) curves for the two data sets for various scenarios, including picking the strongest amplitude position only, choosing all samples exceeding a minimum response amplitude, and using samples within a distance range. The results showed that EMIS discrimination underwater can be effective, but the air results were better – perfect when using only the maximum sample point. Part of the degradation may result from spectral distortion of the target data from the CCR and propagation effects, including the quadrature frequency windowing, and there is also data quality issues related to the environment, including wave noise and background sensitivity to the water surface (tidal drift) and nearby objects (i.e., the experimenters body in the vicinity of the sensor gives a negative CCR). Comparing the ROC curves for the free-air using all ten versus windowed (only eight) quadrature data showed no appreciable difference, indicating that windowing for underwater missions does not jeopardize the potential for EMIS discrimination.

The first attempt to collect data for the discrimination study, with the sensor moved over a chipboard template and within a foot or two of the surface, demonstrated the spectral sensitivity to the air interface and non-conducting objects when very near the sensor coils. These issues, particularly in very shallow water, will probably be of greater concern in marine missions than spectral distortion from CCR or propagation effects.

Objective

The marine mission entails both fundamental differences in the EMI response of a metal object immersed in a conductive host medium as well as operational considerations for data acquisition in a marine setting. The former requires a quantitative understanding of the effects of the seawater on the GEM-3 spectral response to UXO for various sensor-target geometries and target

characteristics, and the latter requires some practical system and platform design and prototyping.

The project focused on the underlying phenomenology relating to the effects of the conductive seawater on the EMI response in general and specific to the GEM-3 sensor. The approach included the development of modeling algorithms that included seawater effects on EMI responses of UXO with subsequent model studies to elucidate and quantify the important physics associated with the problem, and experiments to demonstrate these effects. The phenomena of primary interest were the CCR and skin-depth propagation that distort the spectral response of the target. This is of primary importance in the context of EMIS discrimination that depends on characterizing the target using its spectral signature. Also, the potential for exploiting the CCR to extend the detection range was studied.

Other important practical aspects of underwater EMI that were studied were noise related specifically to the marine environment and the interfering response of non-conductive clutter arising out of the CCR from insulting objects immersed in a conductive host medium. These issues were addressed.

A discrimination test completed the experimental suite, in which surrogate UXO and clutter were targets in a controlled underwater experiment, and a simple EMIS based algorithm utilized to compare discrimination with a free-air control experiment to evaluate the potential performance of broadband EMI for clutter discrimination in a marine setting.

Platform concepts were designed, and one with what we ascertained to have the best potential for a practical system was fully developed and subsequently used in the San Francisco Bay for a Navy cleanup project.

Background

The GEM-3 broadband electromagnetic induction (EMI) sensor (Won, et al., 1997) has demonstrated its potential for UXO/clutter discrimination over land. There is a corresponding need for shallow marine environments in which the sensor would operate submerged in seawater and the targets either lie on the bottom or buried in seawater-saturated sediments. This poses unique challenges for technologies used to detect potential UXO and distinguish between UXO and other debris, both in terms of the actual response from these targets to the sensor, and in terms of the data acquisition challenges encountered when working in a marine environment.

Past experience in underwater UXO detection research is limited; Geophex conducted a trial survey in the prove-out area at Mare Island in the San Francisco Bay in 1999. Two special-made single GEM-3's were configured to be submerged at the ends of PVC tubing rigidly mounted vertically from the ends of a crossbeam attached to a rubber pontoon boat. The GEM-3 sensors' primary fields interfered with each other, so only a single sensor could be deployed, and a magnetometer replaced the other. This simple test succeeded in showing that a GEM-3 could detect UXO in shallow water.

Materials and Methods

The two aspects of this research consisted of computer modeling and analysis, and experiments in shallow seawater. The methodology for the computer modeling was to develop analytic algorithms for special cases that would provide insight as to the fundamental physics related to the EMI response of a metal object when immersed in a conductive host medium as well as quantify the effects of seawater that would allow prediction of the spectral distortion of the GEM-3 response to UXO in seawater. The special cases included finitely conductive and permeable spheres in a conductive background, spheres encased in a shell (2-layered sphere) with different conductivity and/or permeability immersed in a conductive background, and infinitely conductive (or insulating) spheroids immersed in a finitely conductive background.

The experimentation provided confirmation of the modeling as well as measurements for UXO-like objects that could not be modeled. We also encountered noise unique to the marine environment that can be anticipated to be an issue in operational surveys, and we have a better understanding of these noise sources and the impact on data.

We performed a series of controlled experiments in which broadband GEM-3 EMI data were collected for a number of targets at various distances and orientations. The first two sets of experiments were aimed at demonstrating the salient effects of the seawater on the spectral EMI response of these targets and provide a firm understanding of the physics involved. We also wanted to learn the appropriate adjustments that are needed to the sensor parameters (i.e. frequencies used, sensor-target geometry restrictions for target classification) when working in seawater. The setup for the first experiment was simple, but with marginal control on target position and orientation (Figure 1); the second setup employed an indexed linear platform that improved the control (Figure 2).

We conducted the final set of experiments to test the viability of EMIS based discrimination in seawater. Our first attempt to collect spatial samples over a two-dimensional grid was problematic. Our first attempt to achieve this used a chipboard platform with small holes in which the sensor was to be positioned with an attached peg. This setup did not provide quality data and was difficult to use under water. The chipboard was difficult to position under water because it floated and it was pushed up and down by moderate water motion. We managed to collect data with the target below the platform, moving the GEM-3 coil from point to point by hand, and collecting background with the coil off the platform edge.

With this setup, the sensor was relatively close (~8” – 1.5’ depending on tide) to the water surface, and the background did not have the chipboard against the coil. It turns out that the quadrature response at the highest frequency used (21690 Hz) to the board is –500 ppm, which we subsequently confirmed by computer modeling. At that sensor depth, wave noise, and background sensitivity to depth the sensor was held, degraded data above a kilohertz.

In a second go-around, we collected data at well-controlled target positions and orientations using an indexed grid platform and target jigs that fit into the index slots (Figure 3) with the sensor attached to the frame below. We used surrogate UXO items that encompassed a range of sizes appropriate, and a suite of clutter items (Figure 4).

Figure 1. First experimental setup showing the GEM-3 mounting frame placed in water and the underwater GEM-3 (left), and a measurement being made (right) with only rough control of the target position and orientation.

Figure 2. Second experimental setup showing the GEM-3 mounting frame placed in air (left), and in water (right), showing improved target-sensor geometry control.

Figure 3. Final experimental setup showing the GEM-3 mounted on the frame below a target mounted on a jig that fit on rails with positioning slots in air (left), and in water (right), providing precise target-sensor geometry control over a 2-dimensional grid.

Figure 4. Targets used for the discrimination experiment, with seven surrogate UXO covering a wide range in size (right side of photo), and seven clutter items of various form.

Results and Accomplishments

Modeling Algorithm Development

In order to provide a framework for understanding the phenomenology of the effects of conductive seawater on the EMI spectral response to UXO, and to provide a tool for experimental analysis, we devoted the initial phase of the project to developing modeling algorithms for a solid sphere, and a sphere surrounded by a layer of differing electric and magnetic properties, immersed in a conductive media and interrogated with GEM-3. The math followed the methodology of March (1953). We also coded a half-space algorithm for quantifying sensitivity to depth variations (or waves) from the air-water interface.

The sphere algorithms, complex in detail, show a separation of the response from two distinct phenomena, described by mineral exploration geophysicists (e.g., Lajoie et al., 1976) as the eddy current response (ECR) and current channeling response (CCR). The former exists in the free-air case, but modified by the retarded potential, or propagation effects associated with the skin depth of the seawater resulting in attenuation and phase rotation that increases with frequency and distance. The latter only exists in the conductive medium case, because it relates to the perturbation to the currents induced in the background medium by the presence of an object of different conductivity (currents are channeled and enhanced through a good conductor, and diverted around an insulator). In the free-air case, this term in the solution corresponds to the electric polarization mode, which does not give rise to an induction coil sensor response because the currents are suppressed by the insulating boundary and their poloidal geometry traps the magnetic field.

Noting that the analytical solution for the immersed sphere predicts a slower falloff with distance for the CCR (r^{-5}) than the ECR (r^{-6}) and increases with frequency faster than ECR by a half order, we anticipated a potential increase in detection range from CCR. Using the sphere algorithm, we quantified the point at which the CCR exceeds the ECR for a metallic sphere was a range of about a skin depth (Figure 5). This gain can only be realized if there is adequate signal/noise ratio (snr) at that range, which would be explored in subsequent experiments.

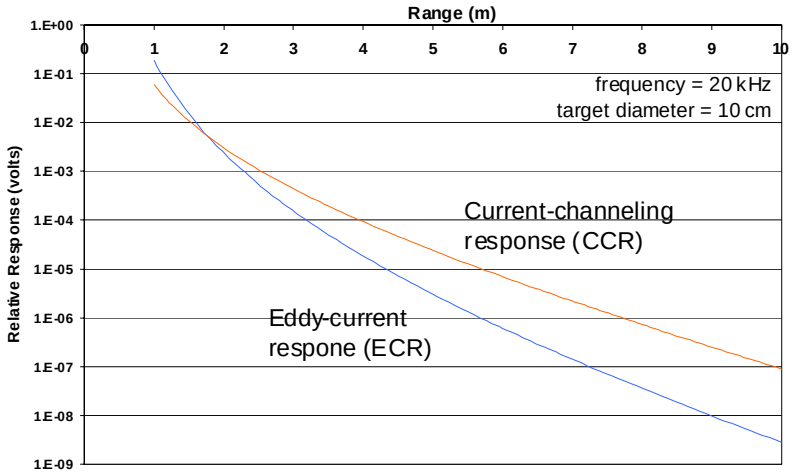

Figure 5. Comparison of ECR and CCR as distance increases shows CCR exceeding ECR at ~1.8 m; one skin depth =1.76 m at this conductivity and frequency.

Later in the course of the project, we developed an algorithm for the response of an infinitely conductive spheroid immersed in a conductive medium and excited by a uniform primary field. This was useful for quantifying the orientation effect on the CCR for elongated (UXO-like) objects. We showed (Figure 6) that the ratio of the transverse to longitudinal primary electric field response was the same as the ratio of the free-air quasi-dc magnetic polarization response to an infinitely permeable ferrous target (computed from solution presented by Das et al., 1990).

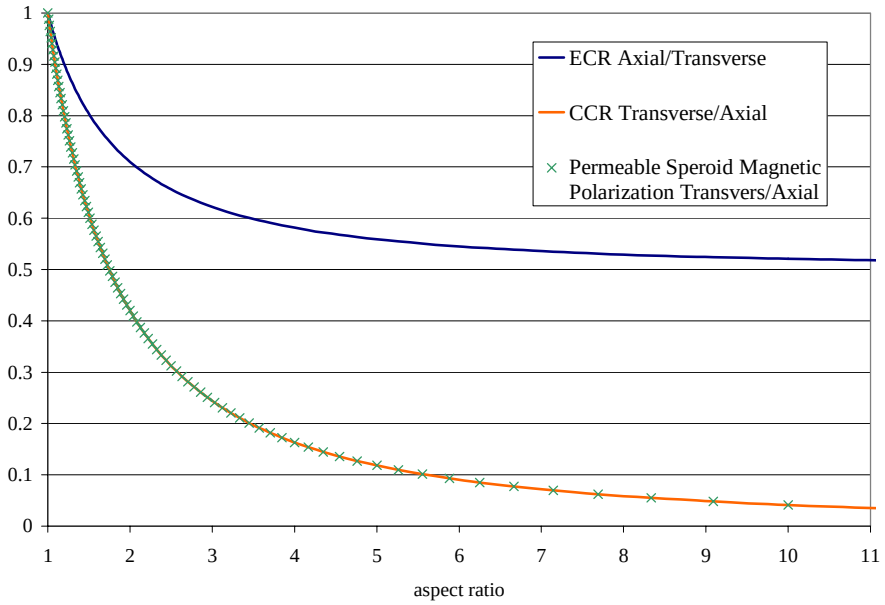

Figure 6. The ratio of axial to transverse response of a perfectly conducting prolate spheroid for various aspect ratios shows the ECR (or CCR for a void) saturating at 0.5, while the transverse to axial CCR decreases towards zero; the latter matches the DC infinitely permeable spheroid polarization ratio.

For the GEM-3, this tells us that when a UXO is near the plane of the coils (lateral distance > depth) and oriented with long axis perpendicular to the line to the GEM, so that the background currents are parallel to the long axis and relatively strong, the CCR will be strongest. A long, thin item will have negligible CCR when the background currents are transverse to the target axis.

Experimental Demonstration of the CCR and Propagation Effects

The first set of experiments focused on a demonstration of the CCR and propagation effects predicted by the analytical models, and the examples (Figures 7 and 8) compare measurements and model fits underwater and in air for a stainless steal 3” diameter sphere. The depths are slightly different between air and water, so the air spectra were scaled to match at low frequencies, showing the spectral distortion from the seawater in the high-frequency quadrature. The sphere conductivity and permeability were found by fitting the air data, and the seawater conductivity by fitting the underwater data. The zero-offset (target directly above sensor along coil axis) case has no CCR, and the propagation effect tends to push the high-frequency

quadrature negative, whereas the half-meter offset case (at about 0.3 m height) shows CCR that more than offsets the propagation and increases the high-frequency quadrature.

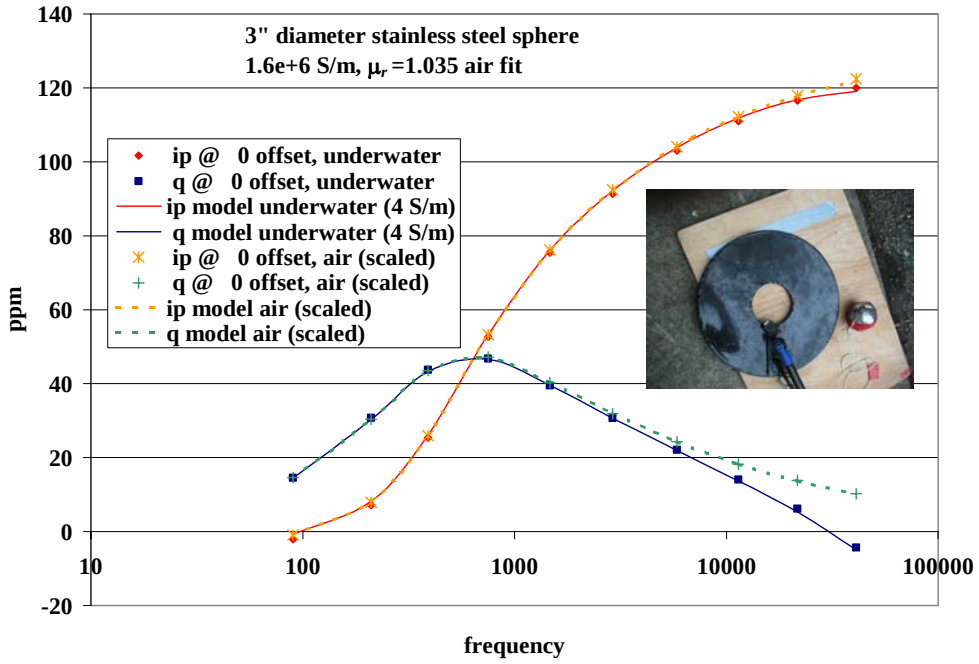

Figure 7. Comparison of measured and modeled GEM-3 spectral response of a stainless steel sphere underwater and in air 35 cm directly above sensor confirms predicted negative propagation effects from seawater on the high-frequency quadrature.

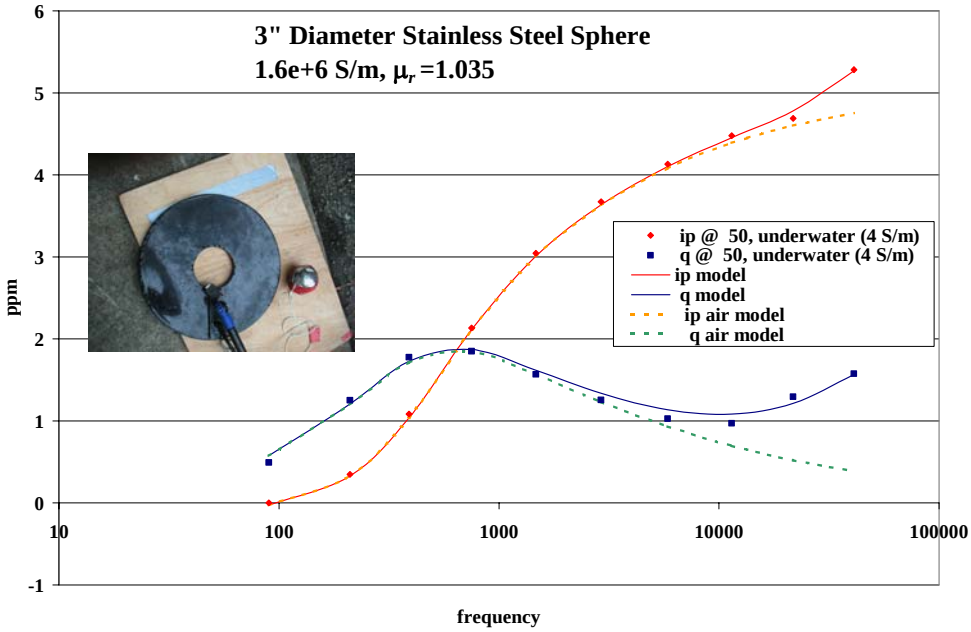

Figure 8. Comparison of measured and modeled GEM-3 spectral response of a stainless steel sphere underwater and in-air model 30 cm above and 50 cm lateral offset confirms predicted CCR effects from seawater on the high-frequency quadrature.

An example of these effects on a UXO-like target (steel pipe) clearly shows the orientation dependence of CCR for large aspect ratio targets (Figure 9).

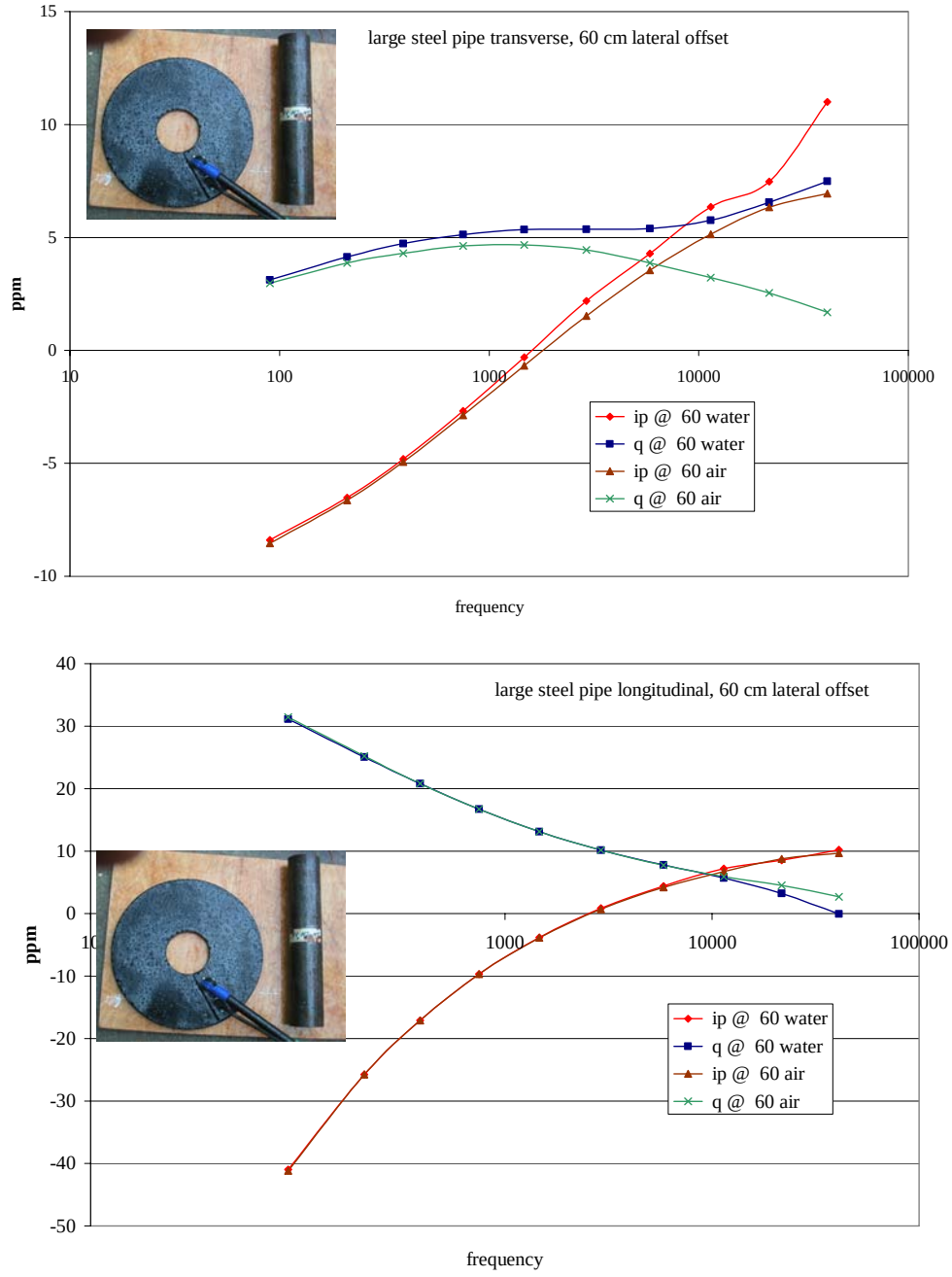

Figure 9. An example of the spectral distortion from the effects of seawater for a large steel pipe with the target lateral offset (60 cm) somewhat greater than depth (48 cm). When the long axis of the target is along the background current direction (transverse to sensor radial), current channeling distorts the high frequency response, particularly the quadrature component (top), whereas propagation effect is greater than CCR for the perpendicular orientation (bottom).

We encountered measurements lacking the predicted CCR with both a 12 lb steel shot put in our first experiment and a 16 lb steel shot put in the second. The first, on inspection, had been painted, and a thin insulating skin could be shown to alter (suppress or even reverse the sign) of the CCR; the second had the paint ground off, but the CCR had similar suppression, leading to the conclusion that the surface was sufficiently (though not visually obvious) corroded to create a similar insulating skin. In Figure 10 we show a comparison of measurements from the second experiment for the 16 lb shot put, and models with and without a corroded skin, at a height of 13 cm and offset of 51 cm. This result implies that painted and/or corroded UXO may exhibit weak or even negative CCR, but if portions such as the nose and tail are not insulated, the CCR similar to the pipe in Figure 9 may still occur.

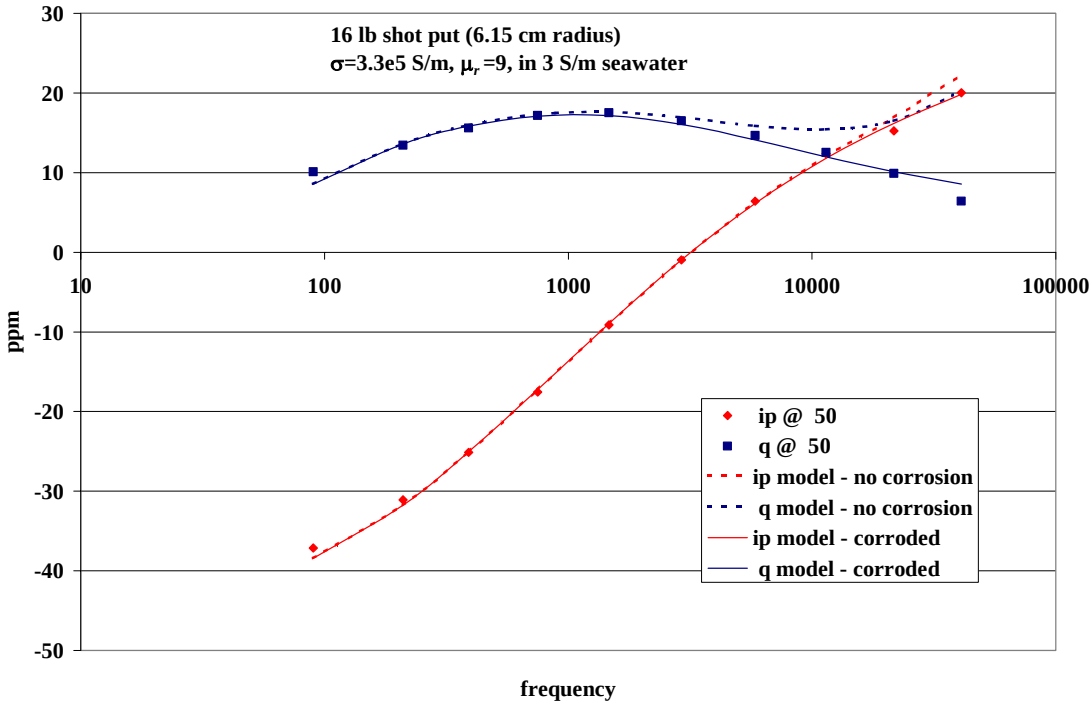

Figure 10. Comparison of measured and modeled GEM-3 spectral response of a shot put 13 cm above and 50 cm lateral offset cannot be modeled as a simple sphere in conductive seawater, which predicts CCR enhancement of the high frequency quadrature, but adding a thin poorly conductive corrosion skin (0.5 mm, .025 S/m). The shot put parameters were derived by fitting free-air spectra.

We present another example that illustrates both the orientation dependence of CCR on an elongated target, and the effect of an insulating layer, in Figure 11. This particular case uses a non-ferrous (aluminum) pipe, which has the interesting property that the free-air (ECR) response is independent of orientation, and reaches the inductive range (strong flat inphase, well above quadrature peak) at a low frequency. Since the quadrature ECR is weak, the CCR stands out. Note that “transverse” and “longitudinal” are with respect to the profile line, and that the transverse case has long axis parallel to background current induced in the seawater. The spectra are similar at low frequencies (dominated by ECR), the CCR is strong for the transverse case, but

insulating the target results in a weak negative CCR. The plastic wrap was punctured at the ends for the attachment cord, so that some current could leak into the target and produce a weak positive CCR for the transverse orientation. Also, from Figure 6, the negative CCR for an insulator is stronger in the orientation with long axis perpendicular to the host current (impedes current flow more than when parallel to current).

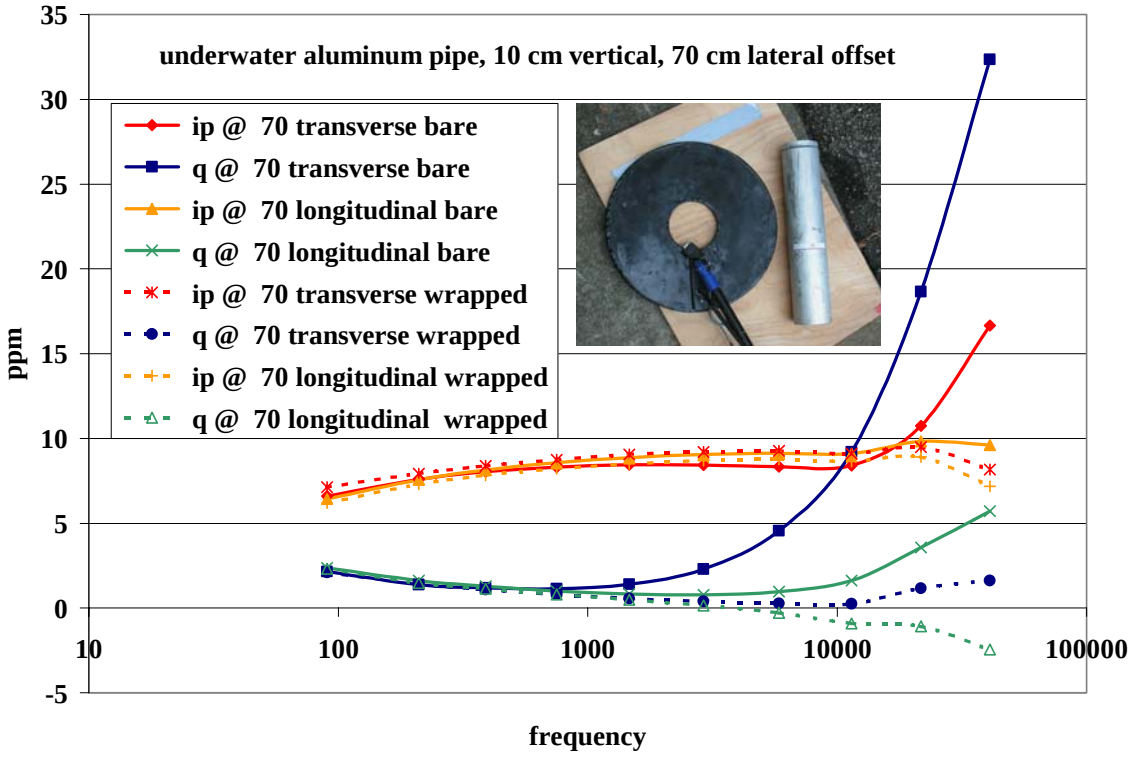

Figure 11. Comparison of measured GEM-3 spectral response of aluminum pipe 10 cm above and 70 cm lateral offset for orientations with axis along current flow (transverse) and perpendicular to current flow (longitudinal) when bare and wrapped in a plastic (insulating) bag shows similarity of the inphase response at all but the highest frequency but strong CCR above a few kilohertz for the bare transverse case. Insulation suppresses the CCR (and is negative if the insulation is perfect); the ECR for non-ferrous pipes is independent of orientation.

Many more examples of the CCR and ECR for various targets and geometries were presented in quarterly and annual reports, and IPR's and the SAGEEP conference.

Potential Increase in Detection Range from the CCR

For the 40 cm (diameter) coil GEM-3, we quantified the benefit in terms of detection footprint resulting from the slower distance falloff of the CCR than the ECR as described above. The key question pertains to actual sensor snr – the benefit can only be realized if the signal is detectable at the range where the CCR is comparable or greater than the ECR, which is approximately one skin depth (1.76 m in 4 S/m seawater at 21690 Hz).

Although we use several different multi-frequency detection algorithms, one of the simplest that we have used extensively is a simple sum of the quadrature responses over all frequencies (Qsum).

We compare Qsum profiles from 30 cm to 100 cm for the large steel pipe in transverse and longitudinal orientations in air and water in Figure 12. For this ferrous target, the ECR has a large quadrature component, especially in the longitudinal mode, and the detection range extends out to 90 cm lateral offset at the 46 cm height for the longitudinal orientation. The transverse mode ECR is somewhat weaker, and in air the detection range is about 10-20 cm less, but in water, the CCR increases the Qsum enough to bring it back to the 90 cm range. This is not a drastic difference but it could help some.

The case for the non-ferrous aluminum pipe (Figure 13) is different, because the ECR is near the target inductive limit at much lower frequencies, which means the ECR is primarily an inphase response and the Qsum detection range is less than for the comparable size steel pipe. The CCR is substantial for the transverse orientation and is evident even at 30-40 cm offset; at 60-70 cm the CCR substantially increases the s/n and increases the detection range to 90-100 cm for that orientation.

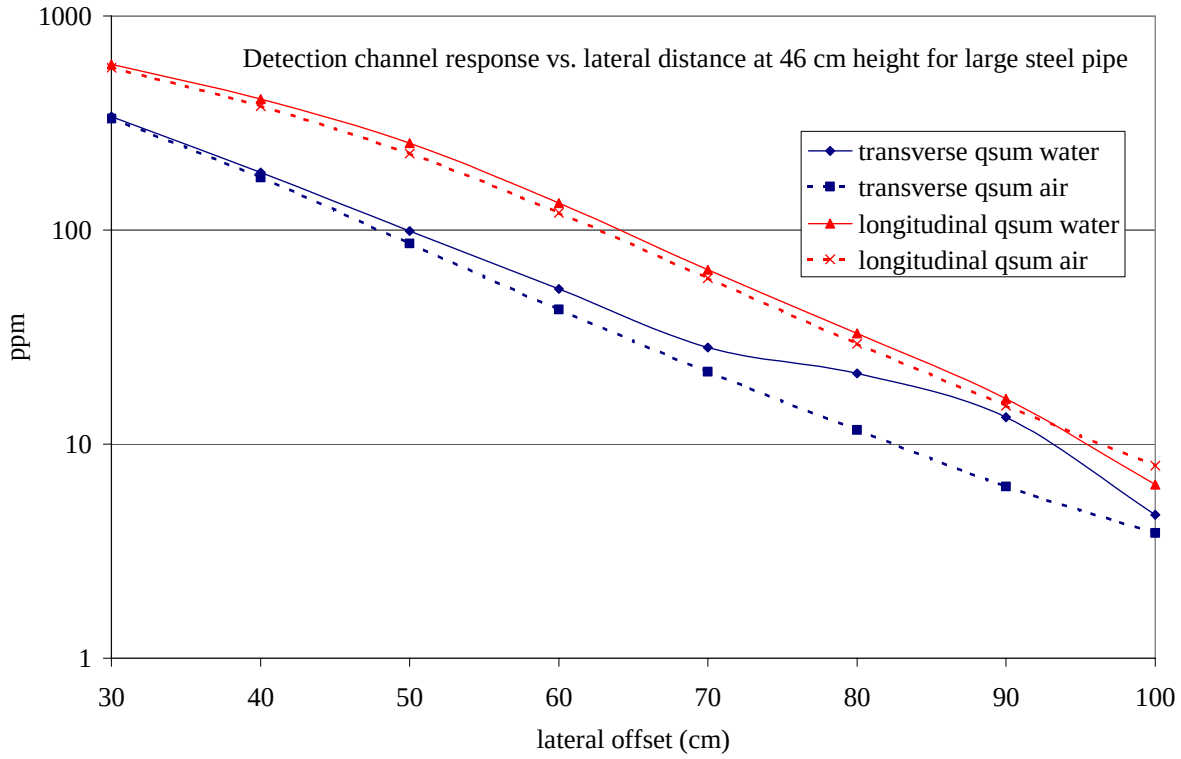

Figure 12. QSUM detection channel response (note log scale) falloff with distance for the large steel pipe at just under a half meter height shows no benefit if the orientation is poorly coupled to CCR, and a marginal increase from about 80 cm to 90 cm when optimally coupled for CCR (note that the ECR is more optimal when the CCR is weak, and the CCR "equalizes" the footprint for the two orientations).

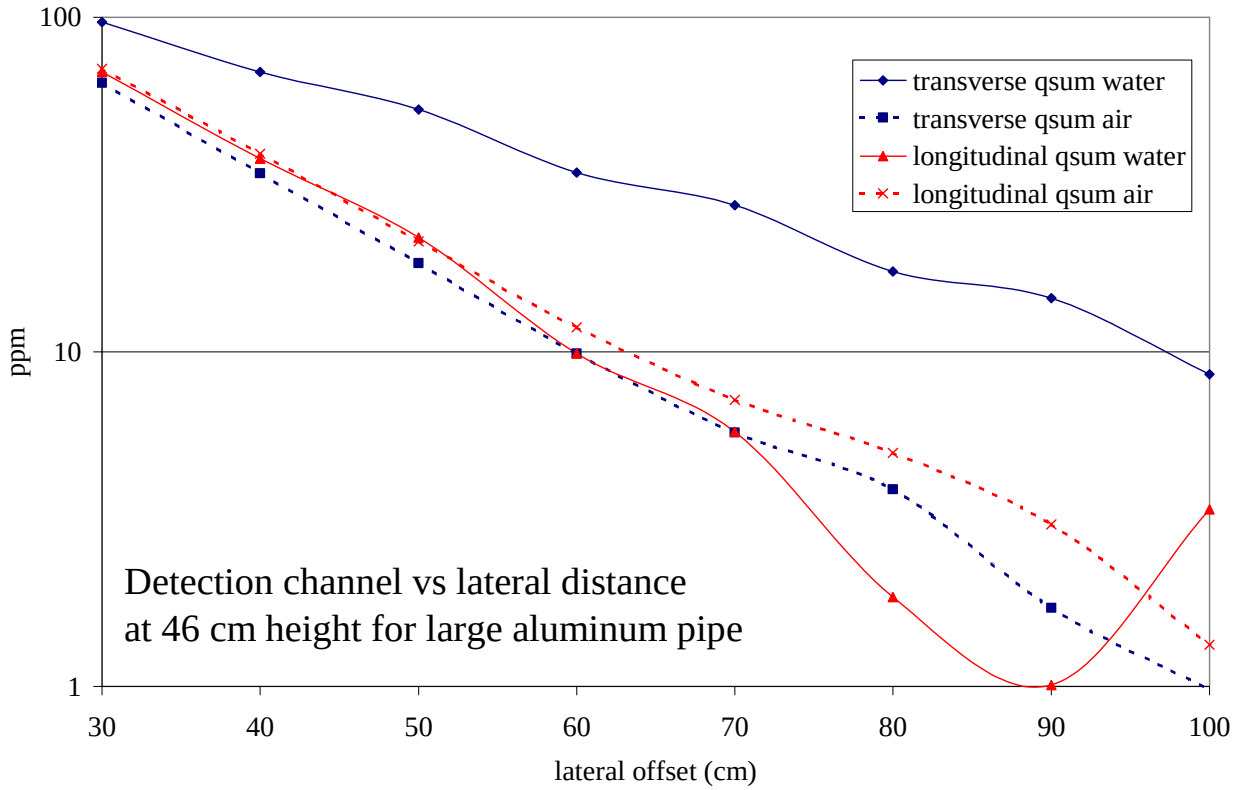

Figure 13. QSUM detection channel response (note log scale) falloff with distance for the large aluminum pipe at just under a half meter height shows no benefit if the orientation is poorly coupled to CCR, but a significant increase from about 60 cm to 90 cm when optimally coupled for CCR (note that the ECR for non-ferrous pipes is orientation independent and weaker than steel).

When the sensor height over the target is reduced, the relative CCR enhancement increases somewhat. If a UXO were painted or corroded to the point in which the CCR is suppressed, then obviously any footprint benefit would be lost. We do not have enough experience with actual UXO in a marine setting to conclude whether in fact most will have corroded to the extent that CCR will not be a factor; if the rust is porous, the CCR may persist. Non-ferrous UXO may be easier to detect in seawater because they may suffer less corrosion and because their ECR is weaker and they are more difficult to detect underground.

The Impact of Spectral Distortion from Seawater on EMIS Based Discrimination

Our algorithms for determining whether a target is likely UXO or clutter using GEM-3 data are mostly based on matching the spectra to a library of known UXO spectra, and if the goodness of fit to the best match is poor, declare the target clutter. The spectral matching technique has been termed electromagnetic induction spectroscopy (EMIS). We have developed other approaches, such as determining aspect ratios (i.e., prolate is UXO, oblate is clutter), but we have not applied them in any of our demonstrations or surveys, and they will not be considered here.

The first question that comes to mind concerning applicability of GEM-3 EMIS in the marine environment is whether spectral distortion from mixing the CCR with the ECR in unpredictable proportions and propagation effects will degrade the spectral matching to an unacceptable degree.

For our assessment of EMIS performance we processed with our simple single-point matching algorithm independently for each position sample. This algorithm, which matches a measured spectrum to the best-fit linear combination of the library spectra for the vertical and horizontal UXO orientations, has the advantage that position information is not required, and that a large set of spatial samples are not needed for inversion (Norton et al., 2001). The disadvantage is that it does not provide a means of utilizing multiple samples with position information to better resolve the target character. But an assessment of this simple algorithm should elucidate whether the EMIS concept is inherently inapplicable to marine missions even if more complex algorithms were used.

First we processed the data collected during our second underwater experiment using a library collected in air. Since both the spectral distortion from CCR and propagation and the noise from waves and tidal drift affect the high frequencies (described in the next section), we excluded the highest two frequencies, limiting the range to 11450 Hz. The results, summarized in Table 1, are encouraging. In general, when the snr is reasonable (i.e. target within a half meter lateral distance), the spectral match identifies the correct item even though underwater data were matched to in-air library spectra. The goodness-of-fit was also significantly worse for the clutter item (a metal paint tray) than for any of the ordnance, showing promise in terms of clutter discrimination. The non-clutter item that consistently gives the poorest fit, though correctly identified, is the large aluminum pipe; non-ferrous targets may be more distorted by the seawater.

Table 1. Spectral Matching Algorithm Performance

position (cm)	ssball	ssball in tupperware	shotput	shotput repeat	m1-2-5 long	m1-2-5 trans	m3-4-7 long	m3-4-7 trans	al52 long	al52 trans	clutter - paintray
0	0.048	0.025	0.023	0.025	no data	0.019	no data	0.019	no data	0.073	0.540
10	0.040	0.026	0.023	0.022	no data	0.019	no data	0.018	no data	0.082	0.764
30	0.043	0.033	0.016	0.015	0.018	0.021	0.011	0.013	0.165	0.109	0.465
40	0.066	0.072	0.018	0.013	0.018	0.026	0.009	0.023	0.156	0.133	0.377
50	0.167	0.131	0.018	0.011	0.014	0.048	0.009	0.041	0.136	0.188	0.289
60	0.287	0.353	0.042	0.026	0.009	0.094	0.015	0.070	0.120	0.332	0.235
70	0.526	0.538	0.121	0.070	0.024	0.105	0.026	0.136	0.144	0.560	0.216
80	0.376	0.407	0.271	0.098	0.035	0.243	0.043	0.167	0.243	1.100	0.216
90	7.340	0.663	0.382	0.192	0.052	0.798	0.108	0.393	0.704	1.720	0.233
100	1.310	0.689	0.456	0.413	0.091	1.360	0.295	0.392	0.842	4.030	0.263

Key: numeric value = normalized error of best fitting item
Green => only the correct item error < .05
Blue => correct item error best fit and < .05, but other items also had error < .05
Gold => only the correct item error < 0.1
Yellow => correct item error best fit and < 0.1, but other items also had error < 0.1
No color => all errors > 0.1, correct item is the best fit; clutter, all errors > 0.1
Maroon => all errors > 0.1, correct item not the best fit
Red => error < 0.1 for only incorrect item the best fit

Our final experiment was aimed at a more comprehensive discrimination study, including a broader range of surrogate UXO and clutter items (Figure 4) and target-sensor geometries (Figure 3). We also tailored the spectrum more towards our goal of discrimination in seawater and shifted the GEM-3 frequencies to a 21690 Hz bandwidth – rather than deleting the two highest, we reduced the intervals between them with the intent to make up for bandwidth reduction by increasing the spectral resolution. We also employed separate frequency windows for the inphase and quadrature, allowing full range inphase while reducing the influence of the distorted high frequency quadrature components. However, we first compared this change on the previous data set, and the improvement was not readily apparent even though inspection of the spectral matches looked like it should.

We collected a set of in-air control data with the setup shown in Figure 3 for each of the targets over the 2-dimensional grid at 20 cm intervals and maximum distance along each direction of 60 cm (note, we did not collect a complete 7 x 7 square pattern – instead we collected 3 points at 60 cm offset, 5 points at 40 cm offsets, and 7 points at 0 and 20 cm offsets, for a total 37 positions; we collected background data between each profile and used a linear interpolation removal scheme). The base set of UXO surrogate runs used a jig that held the targets in approximately a 45˚ degree inclination angle. We repeated this procedure with the entire apparatus immersed in seawater (Figure 14).

Figure 14. We collected data with the indexed platform immersed in seawater, with the sensor fixed to the frame underneath the target grid; a target jig that slid along indexed rails facilitated positioning. The larger targets required deeper (higher tide) water than shown.

We also collected additional sets of underwater suites with different target heights and orientations. We used the same in-air library for both in-air control and underwater discrimination tests. In Figure 15 we compare ROC curves for the in-air and base set underwater results, where we have transformed the misfit into a 0-10 confidence ranking. We used the misfit for the UXO surrogates for the actual item even if a better fit to another UXO item occurred, to ensure that UXO/clutter classification assumed only that particular ordnance was included in the library, while the clutter used the best match.

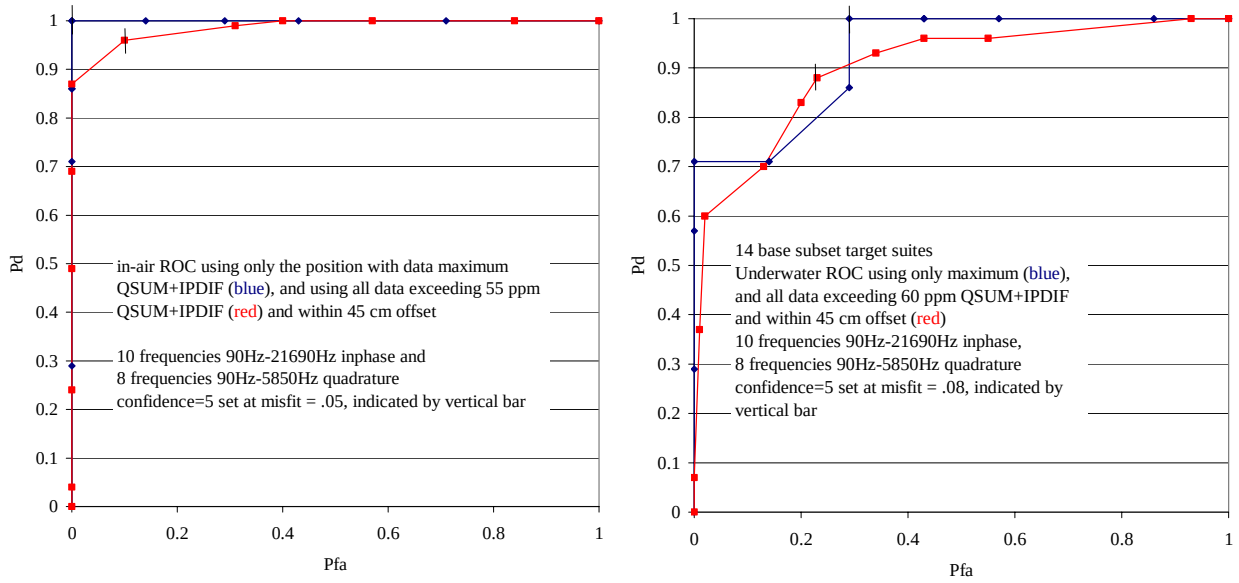

Figure 15. ROC curves for in-air (left) and underwater baseline data set (right), using only the maximum amplitude position sample (blue), and using all samples above threshold amplitude and within 45 cm lateral offset (red). The top two quadrature frequencies were not used.

We include ROC curves that select the peak amplitude position for each target (blue curves) to assess an idealized case were there is always data over the top of the target available, and using all positions within 45 cm lateral offset (up to 17 points) and above a detection threshold (red), indicative of a range of likely closest positions from survey data based on our underwater array with 60 cm coil spacing (30 cm to midpoint).

Based on inspection of the spectral distortion underwater, we initially windowed the quadrature band to 90 Hz – 5850 Hz (not using 11430 Hz and 21690 Hz). We processed the in-air with and without the window and, since there was no significant difference, concluded that little inherent discrimination is sacrificed by cutting out those components. The in-air results are significantly better than the underwater – perfect for the peak amplitude points, but the underwater results nonetheless show reasonable discrimination performance.

On further inspection of the underwater spectra, we found that in some of the weaker amplitude cases, the 21690 Hz in-phase and 5850 Hz quadrature values appeared distorted, and we reprocessed the underwater data with those frequency components windowed out (Figure 16) for the baseline set and the expanded set (baseline one each of 7 UXO and 7 clutter; expanded 17

UXO and 10 clutter – same targets but some new heights/orientations). The expanded set using the original frequency window (not shown) also showed some reduced performance, but not as much as the baseline set.

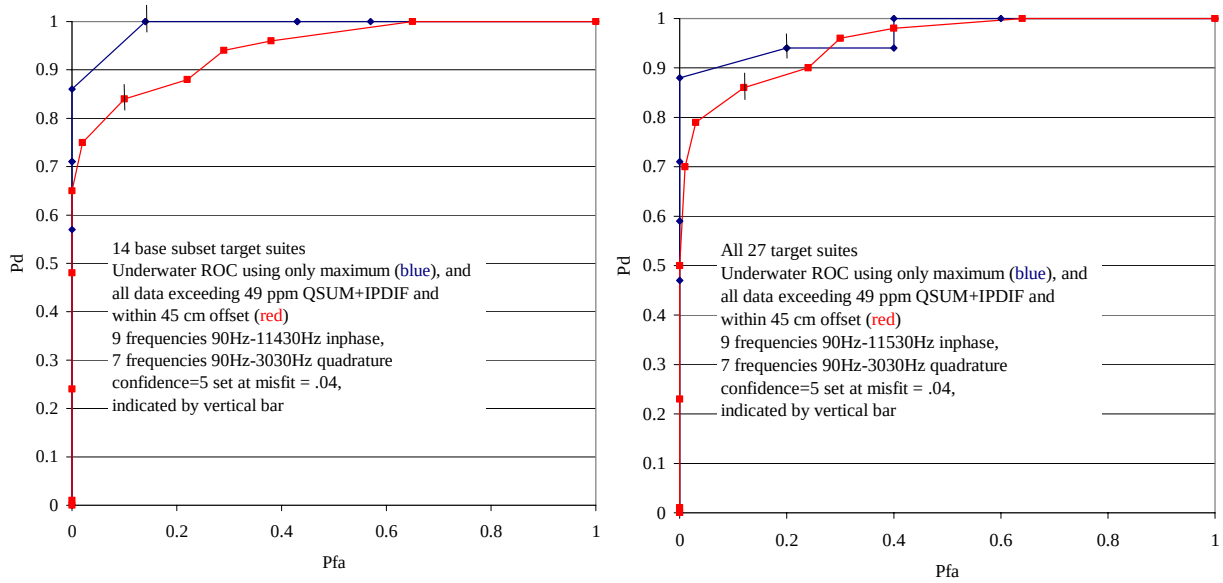

Figure 16. The ROC curve on the left was generated from the same base target set as in Figure 15, but excluding the top three quadrature frequencies and the highest inphase, showing some improvement; the ROC curve on the right includes the extended target sample set. Using the large sample position set (red) shows consistent performance, though the small set using peak values only shows a few of the added target positions were more difficult.

We present some examples of underwater spectra and library fits in Figures 17 – 20, including some of the more difficult targets for classification.

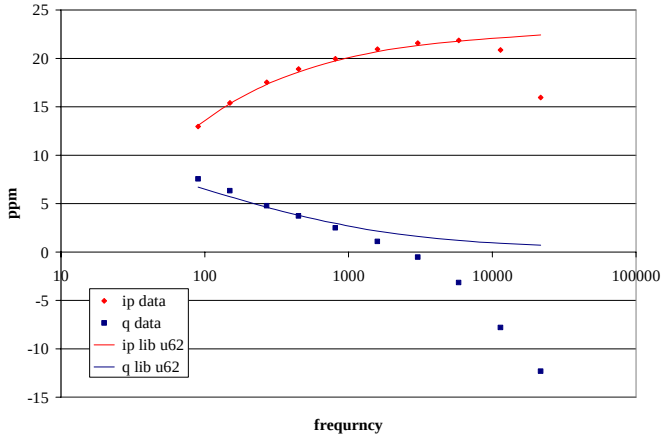

Figure 17. An example of high-frequency underwater spectral distortion resulting in a UXO classified as clutter. This example, at 20 cm lateral offset and 45 cm height, was from the aluminum pipe; non-ferrous ordnance systematically gives larger misfits even though EMIS gives the correct identification.

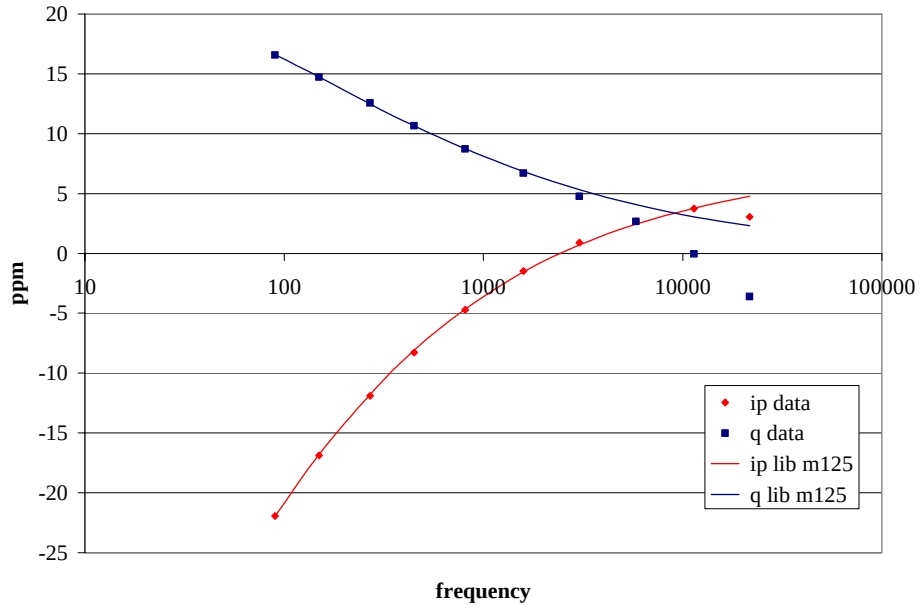

Figure 18. This example of the underwater spectral match of the large steel pipe, at a half-meter height, 40 cm x 20 cm lateral offsets, resulted in a correct classification as UXO and correct specific type identification. The shown fit used the reduced frequency window, but the results were also correct using the original frequencies.

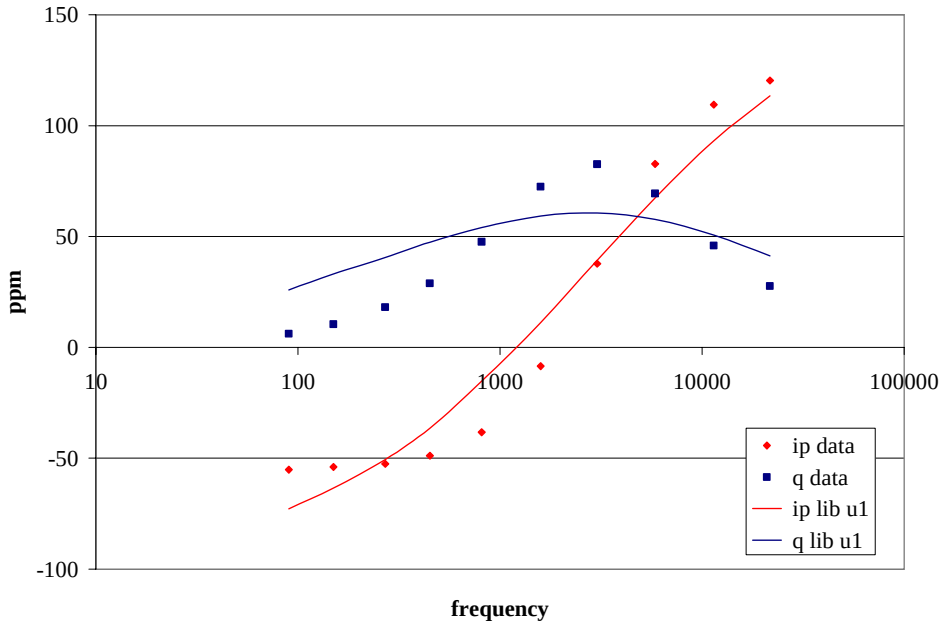

Figure 19. This shows the library best match (medium galvanized steel pipe) to the steel can clutter item directly over the sensor at about 35 cm. This item was definitively classified as clutter using either frequency windows.

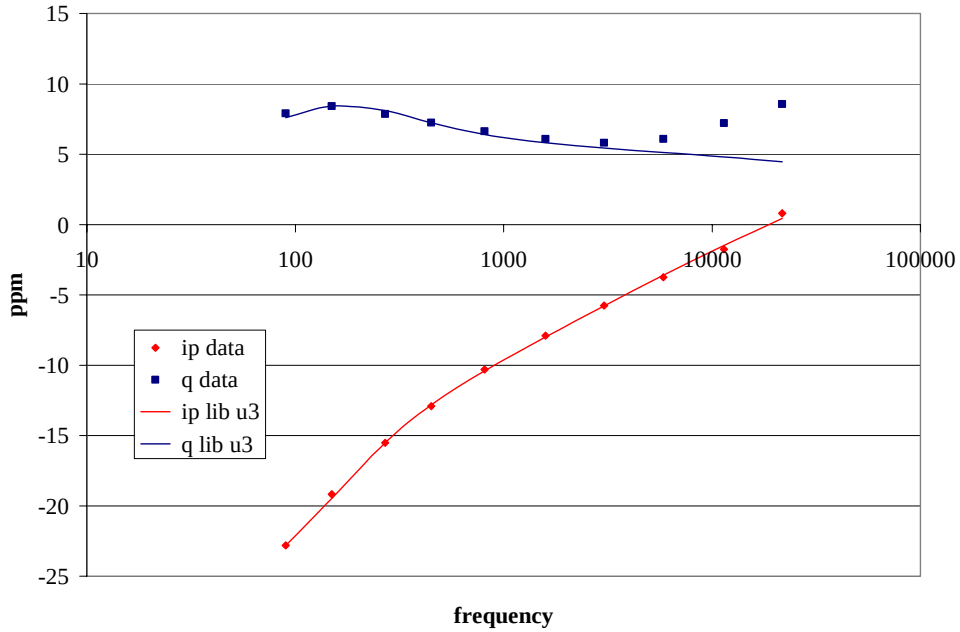

Figure 20. This fit to the small UXO "projectile" of the spectra from the horizontal crowbar clutter at 20 cm x –20 cm lateral offset resulted in a false alarm; in most of the spatial positions it was correctly classified as clutter.

Although there are analysis methodologies that utilize 2-dimensional spatial data (Norton et al., 2001 –2) that may in principle better resolve the target characteristics, we have not investigated them here because we believe that, with current practical underwater acquisition technology, adequate spatial samples with the required data quality and positioning precision simply cannot be obtained from a marine survey.

EMI Data Quality Issues Unique to the Marine Environment

The preceding discussion addressed the effect on EMIS based discrimination from the inherent spectral distortion resulting from the CCR and propagation effects associated with a conductive background medium. There are also aspects of the marine mission that degrade data quality and will impact our ability to characterize the target. In practice, minimizing these noise sources and recognizing them will be important.

The saltwater surrounding the sensor generates a large (820 ppm inphase and 9000 ppm quadrature at 21690 Hz in 4 S/m water) background response that is removed from a target spectrum using background measurements. Perturbations of this background, either temporal or spatial, can distort the resulting target spectrum.

Shallow Water Noise Associated with the Water Surface

In shallow water settings (< 1 m deep), with the sensor mounted on a platform (e.g. sled) that raises it off the bottom (~ 25 cm), the sensor will be within range of the air-water boundary to be sensitive to any variations in the distance or orientation to the water surface. A change from 35

cm to 30 cm depth below the surface results in a change of 25 ppm inphase and 112 ppm quadrature in the background response at 21960 Hz (the effect is approximately linear in frequency). There are two important related sources of noise: 1) waves disrupting the water surface itself, and 2) changes in the sensor depth between measurements over the target and measurements used as background. Even ripples from a moderate breeze can create a serious noise problem as we discovered in our testing (Figure 21). In surf, EMI may not be viable.

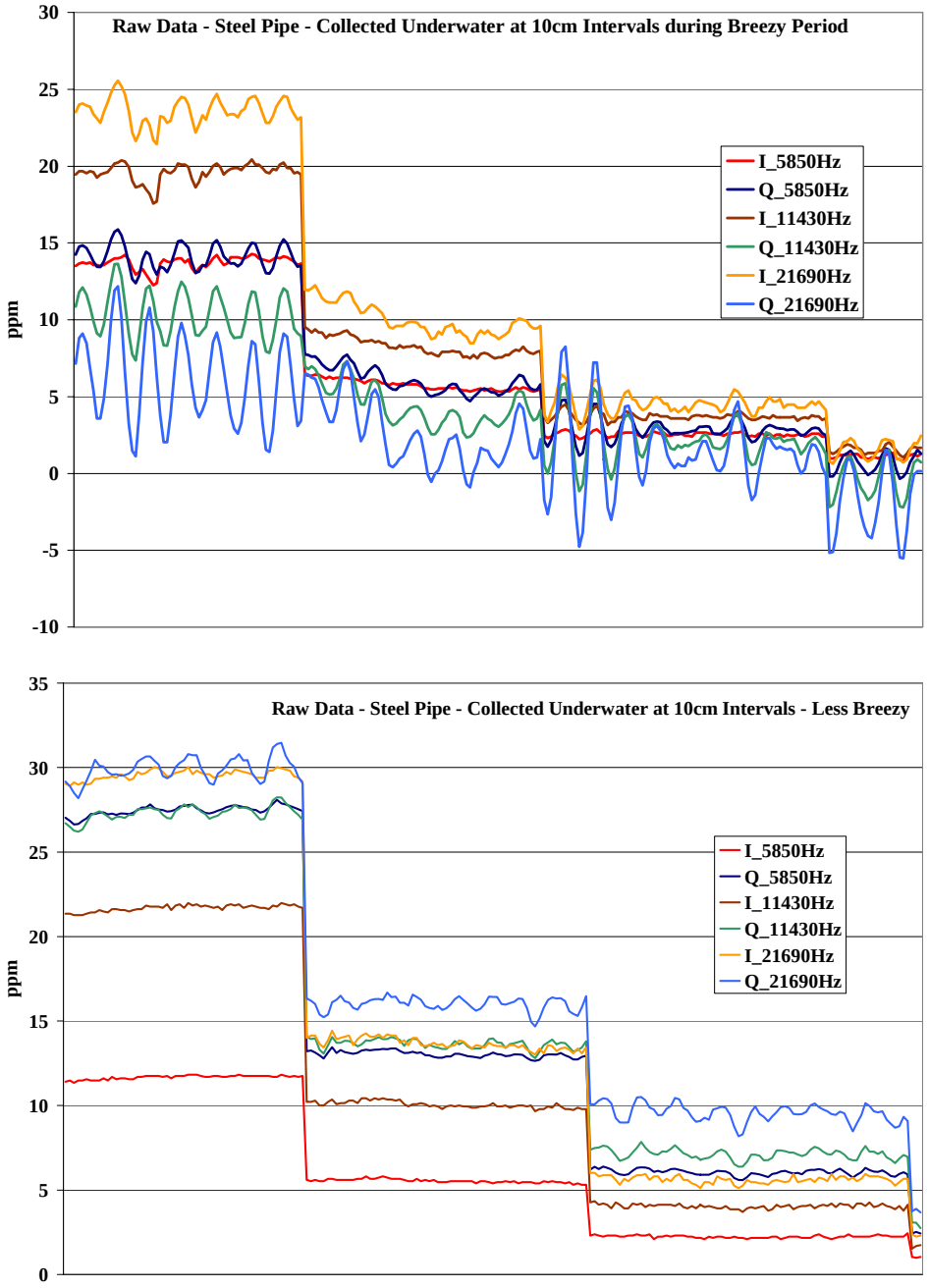

Figure 21. Raw data collected during our first underwater experiment with the sensor about a 40 cm deep shows wave-induced modulation during more (top) and less (bottom) breezy periods superposed on response steps associated with changes in target position.

We confronted the background removal issue during our first attempt to collect 2-dimensional data for the discrimination test, where we moved the sensor from point-to-point on the chipboard platform, taking background readings holding the sensor at about the same depth off the platform. As a background control, we recorded a complete pattern, including off-platform backgrounds, with no target present. A simple line-plot of the two highest frequencies shows the strikingly large response of the chipboard itself, ~ 500 ppm quadrature at 21690 Hz (note that the positive peaks are the background readings between profiles and the chipboard quadrature response is negative; the adjacent shoulders arise from positions with the coil halfway over the board edge). Modeling confirmed that a 1.5 cm thick insulating layer at a 0.5 cm distance will generate the quadrature response shown; the inphase is predicted to be ~25 ppm at 21960 Hz, but also negative; modeling predicts positive inphase if the chipboard is slightly magnetically susceptible. The background stability issue is shown by the variation in the values of the background peaks. This is best explained by slight differences in the depths, and the variation within a peak by motion of the sensor with respect to the surface while holding it free in the water.

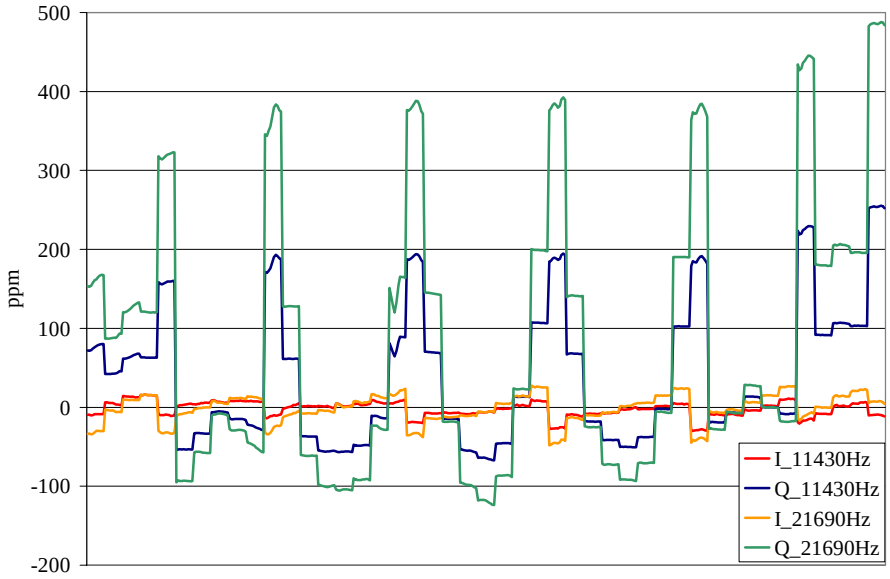

Figure 22. Raw data line plots of data taken with the sensor moved over the chipboard platform grid, with the positive quadrature peaks corresponding to off-platform background (shoulders with sensor hanging off edge). Besides the large negative response of the insulating chipboard, we see inconsistency among and variation during background readings from slightly different sensor depths.

Noise Associated with Bottom and Rock or Non-conducting Objects

In air, rocks and geology give rise to EMI noise primarily from magnetic susceptibility, which manifests in GEM-3 data mostly as an inphase frequency independent spectral shift and can be removed (with some loss of information related to target susceptibility); ground conductivity, except when extreme, has a minor impact on data quality.

In seawater, the situation is quite different. Just as the insulating chipboard created a large negative anomaly as described above by virtue of displacing the conductive water near the coils, a nearby insulating object (including the bottom) will give rise to a negative CCR that increases in amplitude with frequency (Figure 23). In coastal areas where the bottom is rocky, or near manmade structures, even if no metal is present, there can be background noise that can distort the spectrum of a target of interest.

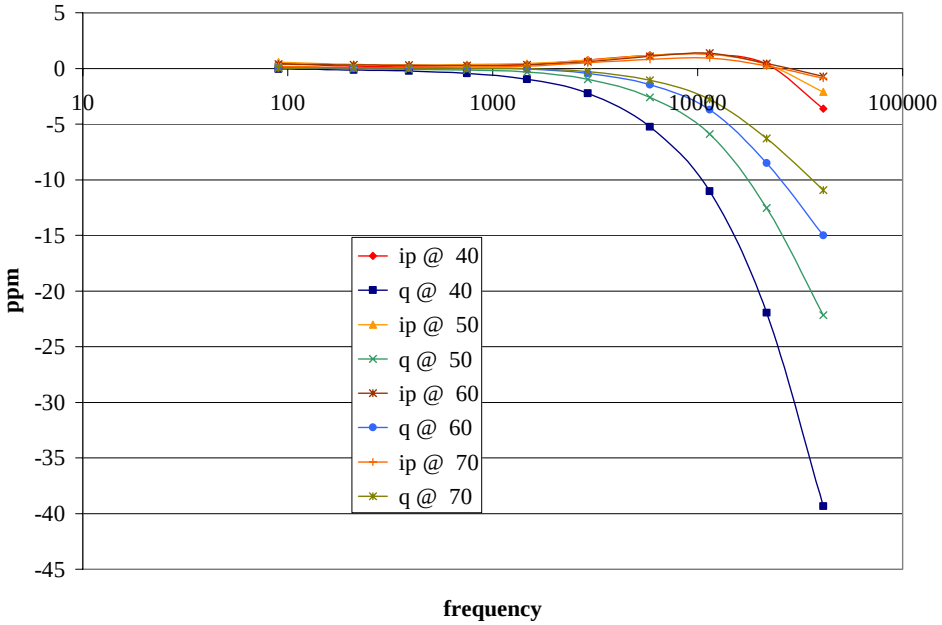

Figure 23. The response of a (water-filled) one-gallon Tupperware container at 20 cm height from 40 cm to 70 cm later distance shows a sizeable negative CCR that could distort the spectrum of a nearby UXO.

An Operational Marine Sensor Array

We built an operation GEM-3 sensor array for underwater surveying and used it in an actual field survey near Mare Island in the San Francesco Bay. We have shown schematics and photos of this system as well as anomaly maps over the prove-out area in previous reports, and Posters at symposiums, and will not duplicate them here. That effort demonstrated success in terms of detection (including many 20 mm targets) and acquisition platform functionality, but not discrimination, which was not a specified goal of the mission. We did learn that target spectral fidelity over a wide frequency range is indeed a challenge for many of the reasons sited above.

Conclusions

We have accomplished the objective at providing an understanding of the phenomenology of EMI in a saltwater medium and elucidating some of the challenges and pitfalls associated with UXO detection and remediation in the marine environment. Although the task will be difficult, and perhaps cannot achieve the same level of success on land, we have shown that fundamentally characterization of UXO and clutter for discrimination with EMI is possible, and specifically, EMIS based discrimination with GEM-3 data viable.

Distortion of the intrinsic target spectra as measured in free-air arises out of CCR and propagation effects related to currents induced in the seawater increases with frequency and distance (lateral distance for CCR, any direction for propagation effects), and for targets within a meter with lateral offset less than height, these effects are generally weak below 10 – 20 kHz, and mostly in the quadrature component, suggesting use of a narrower frequency band than normally used on land.

In operational survey data with the sensor on a moving platform, noise associated with perturbations of the large seawater background response will pose a greater problem than the CCR and propagation effects. These noise sources include wind-induced waves and sensor – surface distance and orientation fluctuations that will modulate the background response, which can be very strong in shallow water zones; they diminish rapidly with depth and at depths greater than a meter will be insignificant. Similar background response perturbations will arise from large nearby (non-conducting) rocks (negative CCR) and sensor motion relative to the bottom. Bottom sediments with a high porosity will have less conductivity contrast and the problem will be reduced. All of these effects increase with frequency and affect the quadrature more than the inphase, and again supports the approach to use frequencies below 10 – 20 kHz inphase and 3 – 5 kHz quadrature.

References

Lajoie, J. J., and West, G. F., 1976, The electromagnetic response of a conductive inhomogeneity in a layered earth, Geophysics, vol. 41, pp. 1133-1156.

March, H. W., 1953, The field of a magnetic dipole in the presence of a conducting sphere, Geophysics vol. 16, pp. 671-684.

I.J. Won, Dean A. Keiswetter, David R. Hanson, Elena Novikova and Thomas M. Hall, 1997, GEM-3: A Monostatic Broadband Electromagnetic Induction Sensor, JEEG, vol. 2, issue 1, pp. 53-64.

S. J. Norton and I. J. Won, Identification of buried unexploded ordnance from broadband electromagnetic induction data, IEEE Trans. Geosci. Remote Sensing, Vol. 39, 2253-2261 (2001).

S. J. Norton, I. J. Won and E. R. Cespedes, Ordnance/Clutter discrimination based on target eigenvalue analysis, Subsurface Sensing Tech. Appl., Vol. 2, pp. 285-298 (2001).

S. J. Norton, I. J. Won and E. R. Cespedes, Spectral identification of buried unexploded ordnance from low-frequency electromagnetic data, Subsurface Sensing Tech. Appl., Vol. 2, pp. 177-189 (2001).

Yogadhish Das, John E. McFee, Jack Toews, and Gregory C. Stuart, 1990, Analysis of an Electromagnetic Induction Detector for Real-Time Location of Buried Objects, IEEE Transactions on Geoscience and Remote Sensing, Vol. 28, No. 3, pp 278-288.

Appendices

A. Supporting Data

Data files from the final (2-dimensional grid) experiment are included with submission of this report (uploaded via FTP) as comma separated variable ASCII files, one file for each grid. These data have pre-processing applied, which includes computing medians from samples at a given position and background removal, providing an inphase and quadrature spectrum for each target position, and x,y grid position. The EMIS library is included. Software for EMIS processing is available on request. Data from earlier experiments are available on request.

B. Technical Publications

Bill SanFilipo, Steve Norton, and I.J. Won, The effects of seawater on the EMI response of UXO, Proceedings of Oceans 2005 MTS/IEEE Washington, D.C., September 2005.

Bill SanFilipo, Steve Norton, and I.J. Won, Broadband electromagnetic detection and discrimination of underwater UXO, Proceedings of the 18th Annual Meeting SAGEEP, April 2005.

Bill SanFilipo, Steve Norton, Haoping Huang, and I.J. Won, Broadband electromagnetic detection and discrimination of underwater UXO, poster, Partners in Environmental Technology Technical Symposium & Workshop, December 2004.

Bill SanFilipo, Steve Norton, Brad Carr, Haoping Huang, and I.J. Won, Underwater detection and discrimination of unexploded ordnance using multi-frequency electromagnetic sensors, poster, Partners in Environmental Technology Technical Symposium & Workshop, December 2003

C. Other Technical Material

None

Additional Materials

Separate graphics files for any figure in any report or publication available on request.